Intermediate Boson. I. Theoretical Production Cross Sections in High-Energy Neutrino and Muon Experiments*

R. W. BROWN†
Brookhaven National Laboratory, Upton, New York 11973

AND

J. SMITH
The Institute for Theoretical Physics, State University of New York at Stony Brook, Stony Brook, New York 11790

(Received 31 August 1970)

We present here the theoretical total cross sections for W-boson production in the reactions $\nu+Z\to Z+W+\mu$ and $\mu+Z\to Z+W+\nu$ for a variety of Z. The emphasis is on the energies and corresponding W-boson masses pertinent to the National Accelerator Laboratory. The effects of the W's anomalous magnetic moment, the nucleon Fermi motion, the Pauli exclusion principle, inelastic channels (in particular, deep-inelastic ones), and the problem of incoherent versus coherent production are all discussed. We also give a critique of some recent high-energy compilations.

I. INTRODUCTION

THIS is the first in a series of three papers dealing with the possibility that the W boson may be found at the National Accelerator Laboratory (NAL). Directing our attention towards neutrino- and muon-induced reactions, and assuming that the W does not interact strongly, we consider here the calculation of total cross sections for W production, which is essentially an extension of previous neutrino efforts[1–6] to higher energies, and of the latest muon work[7] to the general nuclear case. In the subsequent papers, we shall discuss the theoretical angular distributions and energy spectra of the W and the signature muons for both real and virtual W decays. The muon distributions for the virtual decay *vis-à-vis* the four-fermion predictions may give us another way of discovering whether or not the weak boson exists even if it is too heavy to actually be produced.

Long after the first speculations[8] about its existence, the present status of the W is that its mass M_W is probably greater than 2 or 3 GeV/c^2, if it really exists at all. The principal experimental evidence for this lower limit has been provided by the BNL and CERN neutrino experiments[9] which looked for the reaction[10]

$$\nu_\mu+Z\to\mu^-+W^++Z'. \tag{1.1}$$

Here the signature for the process is two muons originating at a point, since the semiweak decay

$$W^+\to\mu^++\nu_\mu \tag{1.2}$$

is very fast—the lifetime is probably less than 10^{-18} sec.[11] The absence of such events for neutrino energies $E_\nu\lesssim 10$ GeV implies that $M_W\gtrsim 3$ GeV/c^2. At NAL, the hope is to push E_ν up around 200 GeV, making it possible to consider $M\lesssim 15$ GeV/c^2. There is additional strong evidence that the aforementioned experimental lower limit is correct (or even too small) from nucleon-nuclei collision studies[12] and from cosmic-ray analysis.[13]

The theoretical *raison d'être* arises initially from the electromagnetic analogy.[8] The nonrenormalizable aspects of current-current interactions are not removed by charged boson intermediaries but the feeling that there ought to be a "carrier" of the weak force has prompted considerable theoretical attention on its con-

* Work performed in part under the auspices of the U. S. Atomic Energy Commission.

† Present address: Case Western Reserve University, Cleveland, Ohio 44106.

[1] T. D. Lee, P. Markstein, and C. N. Yang, Phys. Rev. Letters **7**, 429 (1961).

[2] V. V. Solov'ev and I. S. Tsukerman, Zh. Eksperim. i Teor. Fiz. **42**, 1252 (1962) [Soviet Phys. JETP **15**, 868 (1962)]. This work was done in covariant Weizsäcker-Williams approximation.

[3] J. S. Bell and M. Veltman, Phys. Letters **5**, 94 (1963). There is a printing error in Eq. (5) of this reference. One of the terms should read $-\frac{1}{2}(|\mathbf{Q}|/2K_f)^3$.

[4] G. von Gehlen, Nuovo Cimento **30**, 859 (1963).

[5] A. C. T. Wu, C. P. Yang, K. Fuchel, and S. Heller, Phys. Rev. Letters **12**, 57 (1964); A. C. T. Wu and C.-P. Yang, Phys. Rev. D **1**, 3180 (1970).

[6] H. Überall, Phys. Rev. **133**, B444 (1964). This author employed a covariant Weizsäcker-Williams approximation.

[7] F. A. Berends and G. B. West, Phys. Rev. D **1**, 122 (1970); D **2**, 1354(E) (1970).

[8] H. Yukawa, Proc. Phys. Math. Soc. (Japan) **17**, 48 (1935); Rev. Mod. Phys. **21**, 474 (1949); S. Ogawa, Progr. Theoret. Phys. (Kyoto) **15**, 487 (1956); J. Schwinger, Ann. Phys. (N. Y.) **2**, 407 (1957); T. D. Lee and C. N. Yang, Phys. Rev. **108**, 1611 (1957); R. P. Feynman and M. Gell-Mann, *ibid.* **109**, 193 (1958); E. C. G. Sudarshan and R. E. Marshak, *ibid.* **109**, 1860 (1958); J. J. Sakurai, Nuovo Cimento **7**,649 (1958).

[9] R. Burns *et al.*, Phys. Rev. Letters **15**, 42 (1965); G. Bernardini *et al.*, Nuovo Cimento **38**, 608 (1965).

[10] The possibility of conducting W searches via (1.1) was first discussed by B. Pontecorvo and S. Ryndin, in Proceedings of the Conference on High-Energy Physics, Kiev, 1959 (unpublished). See also M. Schwartz, Phys. Rev. Letters **4**, 306 (1960); T. D. Lee and C. N. Yang, *ibid.* **4**, 307 (1960); Phys. Rev. **119**, 1410 (1960). The antineutrino reaction $\bar{\nu}_\mu+Z\to\mu^++W^-+Z'$ has the same differential cross section (cf. Ref. 1) but is less favorable experimentally.

[11] A discussion of this and other possible decay modes can be found in R. E. Marshak, Riazuddin, and C. P. Ryan, *Theory of Weak Interactions in Particle Physics* (Interscience, New York, 1969), Chap. 7.

[12] R. C. Lamb *et al.*, Phys. Rev. Letters **15**, 800 (1965); R. Burns *et al.*, *ibid.* **15**, 830 (1965); P. J. Wanderer, Jr., *et al.*, *ibid.* **23**, 729 (1969); G. S. Hicks *et al.*, Bull. Am. Phys. Soc. **15**, 579 (1970).

[13] R. Cowsik and Y. Pal, in Proceedings of the International Conference on Cosmic Rays, Budapest, 1969 (unpublished). These authors present evidence based on cosmic-ray analysis that $M_W\gtrsim 5$ GeV/c^2.

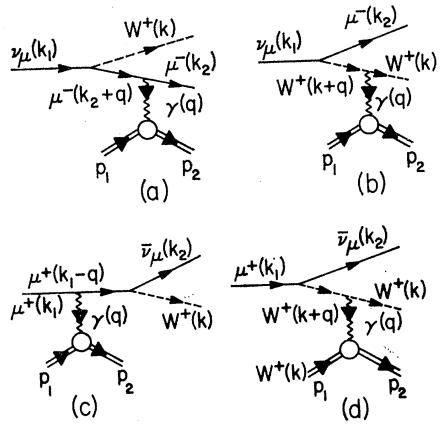

FIG. 1. Feynman diagrams for reactions (1.1) and (1.3).

sequences. Specifically, a number of models[14] indicate that the W's mass ought to lie somewhere between 2 and 10 GeV/c^2. At the very least, the NAL experiments will put these models to the test.

The standard procedure in W searches via (1.1) has been to compare its theoretically calculated values with the experimental result assuming the W to be spin 1—since it couples to $V-A$ currents. In the same sense as current-current calculations, one presumes lowest-order perturbation theory to be a good guide if there is no danger of violating unitarity limits. Taking into account both incoherent and coherent possibilities and using a numerical integration routine, Lee, Markstein, and Yang[1] gave the first theoretical estimates for (1.1) with $E_\nu \lesssim 10$ GeV and iron targets. In this situation, W's of around a GeV or less could be produced. Later, Bell and Veltman[3] numerically inspected the effects of different nuclear form factors and the Pauli exclusion principle, while von Gehlen[4] performed some of the integrations analytically taking into account the Fermi motion of the nucleons. The latter author shows that the asymptotic formula for the total cross section at high energies given in Ref. (1) and the corresponding Weizsäcker-Williams (WW) approximations[2] are not particularly accurate guides here for even extremely large E_ν (2000 GeV). On the other hand, some WW calculations of Überall's agree with those done by Bell and Veltman.

The most comprehensive set of calculations and comparisons with other results has been done by Wu, Yang, Fuchel, and Heller[5] for $E_\nu \lesssim 10$ GeV. This reference serves as a standard for our paper (due to numerical integrations, none of the previous work can be extrapolated to the higher energies of interest here). There is a more recent paper by Berkov *et al.*[15] which reports on larger (e.g., Serpukhov) energies but which is in order-of-magnitude disagreement with what we have found.

Two recent papers[16,17] have dealt with an estimation of the deep-inelastic contributions to W production off of a proton by neutrinos. Their conclusions are in order-of-magnitude disagreement with each other, compelling us to give a third independent calculation. Our results agree with those of Chen.[16]

In addition to the neutrino work, we also perform the analogous calculations for the muon-induced reaction

$$\mu^+ + Z \rightarrow \bar{\nu}_\mu + W^+ + Z', \tag{1.3}$$

a reaction recently advocated[18] as a means of W-searching in view of the energy advantage of muons over neutrinos. Our work considers the general nuclear and deep-inelastic cross sections in addition to extending the proton calculations of Berends and West.[7] The essential result here, reported earlier by Mann and us,[19] is that there is a general difference of two orders of magnitude between (1.1) and (1.3) in favor of the neutrinos for NAL energies.

We begin by writing the lowest-order matrix element and the corresponding differential cross section for (1.1) in Sec. II. Then those integrations which can be done analytically are described in Sec. III, leaving a two-dimensional integral to be done numerically. Section IV contains the numerical results for nucleon and nuclei targets. Section V is directed towards a discussion of the coherent versus incoherent mixing problem and also on the nuclear charge distribution effects as well as the inelastic channels. In Sec. VI we discuss the total cross sections for the muon-induced reaction. In Sec. VII we conclude with a summary of our work. There is an appendix included which contains a trace arising in the spin summation and some intermediate steps in the phase-space integrations.

Since the goal of our paper is to aid experimentalists in future W searches, we have included many of the kinematical details in the presentation and an extensive set of figures and tables.

II. LOWEST-ORDER MATRIX ELEMENT

The lowest-order mechanism contributing to (1.1) and (1.3) involves a virtual photon interaction between the lepton-boson vertex and the target since we assume

[14] S. L. Glashow, H. J. Schnitzer, and S. Weinberg, Phys. Rev. Letters **19**, 205 (1967); R. N. Mohapatra, J. S. Rao, and R. E. Marshak, *ibid.* **20**, 1081 (1968); M. Gell-Mann, M. L. Goldberger, N. M. Kroll, and F. E. Low, Phys. Rev. **179**, 1518 (1969). For further discussion see Ref. 11.

[15] A. V. Berkov, G. C. Bunatyan, E. D. Zhizhin, and Yu. P. Nikitin, Yadern. Fiz. **9**, 605 (1968) [Soviet J. Nucl. Phys. **9**, 348 (1969)].

[16] H. H. Chen, Phys. Rev. D **1**, 3197 (1970).

[17] V. N. Folomeshkin, Institute of High-Energy Physics, Serpukhov Report No. 69-56, 1969 (unpublished).

[18] L. M. Lederman, National Accelerator Laboratory 1968 Summer Study Report No. B. 2-68-74, Vol. 2, p. 55 (unpublished); T. Kirk, National Accelerator Laboratory 1969 Summer Study Report No. SS-11, Vol. 4, p. 191 (unpublished). The μ^- reaction, $\mu^- + Z \rightarrow \nu_\mu + W^- + Z'$, has the same differential cross section (note Ref. 10) but is experimentally less favored.

[19] R. W. Brown, A. K. Mann, and J. Smith, Phys. Rev. Letters **25**, 257 (1970).

that the W does not interact strongly.[20] This means we must specify some electrodynamics: Our Feynman rules[21] follow from the interaction Lagrangian[1,22]

$$\begin{aligned}\mathfrak{L}_{\rm int}=&+e{:}\bar{\psi}_{(\mu)}\gamma_\sigma\psi_{(\mu)}A^\sigma{:}\\&+ie{:}[\partial^\rho W_\sigma{}^*(A^\sigma W_\rho-A_\rho W^\sigma)\\&-\partial^\rho W_\sigma(A^\sigma W_\rho{}^*-A_\rho W^{\sigma*})]{:}\\&+ie\kappa{:}(\partial_\rho A_\sigma-\partial_\sigma A_\rho)W^{\rho*}W^\sigma{:}\\&-g_W{:}[\bar{\psi}_{(\mu)}\gamma_\sigma(1-\gamma_5)\psi_{(\nu)}W^{\sigma*}\\&\qquad+\bar{\psi}_{(\nu)}(1+\gamma_5)\gamma_\sigma\psi_{(\mu)}W^\sigma]{:}\quad(2.1)\end{aligned}$$

to lowest order in $e>0$. Here, κ is a constant signifying the anomalous magnetic moment degree of freedom of the W. In order that the weak interaction reduce to the current-current form at low energies, we identify

$$g_W{}^2=GM_W{}^2/\sqrt{2}\,,\qquad(2.2)$$

where $G\cong10^{-5}/M_p{}^2$ is the Fermi coupling constant for the weak vector current. Here M_p is the proton mass. One further remark about $\mathfrak{L}_{\rm int}$ is that we shall try to take into account all of the strong interactions of the target by way of form-factor fits and accordingly do not explicitly include the target's electromagnetic current in Eq. (2.1).

There is another degree of freedom in the spin-1 boson's electromagnetic interactions that we have not considered in Eq. (2.1) and that is the electric quadrupole ambiguity. A particle of spin S has $2S+1$ intrinsic multipole moments and the three here would be the charge (electric monopole moment), the magnetic dipole moment, and the electric quadrupole moment. It has been difficult, however, to formulate a consistent spin-1 theory which includes the quadrupole degree of freedom[23]; on the other hand, the most reasonable model may be the one which neglects it altogether.[24] Neglecting the extra freedom, the magnetic and quadrupole moments as defined in Ref. 22 are

$$\mu_W=(e/2M_W)(1+\kappa)\,,\quad Q=-(e/M_W{}^2)\kappa\,.\qquad(2.3)$$

With these preliminaries out of the way, the matrix elements, in lowest-order perturbation theory, correspond to the Feynman diagrams in Fig. 1. Our notation for four-vectors is also given in the same figure; in particular, we define the laboratory notation

$$k_i\equiv(E_i,\mathbf{k}_i)\,,\quad p_i\equiv(E_{p_i},\mathbf{p}_i)\,,\quad k\equiv(E_k,\mathbf{k})\,,$$

and

$$q\equiv p_2-p_1\,,\quad p\equiv p_2+p_1\,.$$

Then the square of the c.m. energy and the "momentum transfer" to the target are given by

$$S=(p_1+k_1)^2\,,\quad T=q^2\,,$$

respectively. We shall often use $M_W=1$ units in what follows.

Our interest is focused on the neutrino reaction (1.1) now; comparisons with the muon case are presented later in Sec. VI. In the case of a proton target (we consider targets at rest) for an average over the initial proton's spin and a sum over all of the final spin configurations,

$$d^9\sigma=\frac{1}{32\pi^3}\frac{\alpha^2g_W{}^2}{E_1M_p}\frac{d^3\mathbf{k}_2}{E_2}\frac{d^3\mathbf{k}}{E_k}\frac{d^3\mathbf{p}_2}{E_{p_2}}\delta^4(k_1-q-k_2-k)\mathfrak{F}\,.\qquad(2.4)$$

Here,

$$\mathfrak{F}\equiv T^{-2}P_{\nu\mu}K_{\beta\alpha}L^{\beta\nu\mu\alpha}\qquad(2.5)$$

in terms of the proton trace (and hence the proton electric and magnetic form factors)

$$\begin{aligned}&P_{\nu\mu}=(Tg_{\nu\mu}-q_\nu q_\mu)G_1+p_\nu p_\mu G_2\,,\\&G_1\equiv G_M{}^2(T)\,,\quad G_2\equiv[G_E{}^2(T)+\tau G_M{}^2(T)]/(1+\tau)\,,\quad(2.6)\\&\qquad\tau\equiv-T/4M_p{}^2\,,\end{aligned}$$

the W polarization sum

$$K_{\beta\alpha}=-g_{\beta\alpha}+k_\beta k_\alpha\,,\qquad(2.7)$$

and the lepton trace

$$\begin{aligned}L^{\beta\nu\mu\alpha}=&\,{\rm Tr}\{\boldsymbol{k}_1(1+\gamma_5)[\gamma^\beta(\boldsymbol{q}\gamma^\nu+2k_2{}^\nu)F^{-1}-(\gamma^\beta(2k+q)^\nu\\&+(1+\kappa)(\boldsymbol{q}g^{\beta\nu}-q^\beta\gamma^\nu)+\mu(1-\kappa)(q^\beta k^\nu-k\cdot qg^{\beta\nu})\\&+\mu\kappa(Tg^{\beta\nu}-q^\beta q^\nu))B^{-1}](\boldsymbol{k}_2+\mu)[(\gamma^\mu\boldsymbol{q}+2k_2{}^\mu)\gamma^\alpha F^{-1}\\&-((2k+q)^\mu\gamma^\alpha+(1+\kappa)(\boldsymbol{q}g^{\mu\alpha}-\gamma^\mu q^\alpha)+\mu(1-\kappa)\\&\times(k^\mu q^\alpha-k\cdot qg^{\mu\alpha})+\mu\kappa(Tg^{\mu\alpha}-q^\mu q^\alpha))B^{-1}]\}\,.\quad(2.8)\end{aligned}$$

The muon mass has been denoted by μ and the denominators of the fermion and boson propagators have been called

$$\begin{aligned}&F\equiv(k_2+q)^2-\mu^2=T+2k_2\cdot q\,,\\&B\equiv(k+q)^2-1=T+2k\cdot q\,,\end{aligned}\qquad(2.9)$$

respectively.

We now choose the five independent variables (after integrating over $\mathbf{k}_2$ and E_k via the δ function) for the spin-summed differential cross section to be

$$T,\ U\equiv(p_1-k_2)^2,\ F,\ B,\ \text{and}\ N\equiv p\cdot k\,.\qquad(2.10)$$

Then $\mathfrak{F}=\mathfrak{F}(T,U,F,B,N)$ which is discussed in the Appendix. It was easily handled by an algebraic computer program.

[20] We therefore assume the W to be pointlike in its electromagnetic interactions in spite of its large mass. This is related to the idea that the nucleon and pion form factors are due to hadron clouds whereas the muon without such strong interaction is more like an electron than a pion (although $m_\mu\simeq m_\pi$).

[21] Our basic notation and conventions are those of J. D. Bjorken and S. D. Drell, *Relativistic Quantum Mechanics* (McGraw-Hill, New York, 1964); and *Relativistic Quantum Fields* (McGraw-Hill, New York, 1965). In particular, $\hbar=c=1$, $\alpha=e^2/4\pi$, and $\boldsymbol{p}\equiv\gamma^\mu p_\mu$. The over-all sign on the interaction Lagrangian for spin-1 electrodynamics given in their appendix is incorrect—this leads to some sign errors in their rules. We are indebted to Professor Alberto Sirlin for discussions on this sign problem.

[22] T. D. Lee and C. N. Yang, Phys. Rev. **128**, 885 (1962); T. D. Lee, *ibid.* **128**, 899 (1962). The fields W_σ, $\psi_{(\mu)}$, and $\psi_{(\nu)}$ refer to the W^+, μ^-, and ν_μ, respectively.

[23] Recently Aronson [H. Aronson, Phys. Rev. **186**, 1434 (1969)] found that the inclusion of an arbitrary quadrupole moment would not necessarily violate relativistic covariance.

[24] See T. D. Lee, Phys. Rev. **140**, B967 (1965).

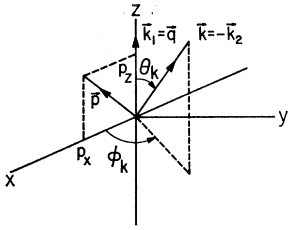

FIG. 2. System of coordinates for the angular integrations.

We describe the phase-space integration in Sec. III. But before getting into that, we ought to mention that our choice of U as an independent is due to the resulting simplification in the transformation to the muon beam case. The two situations differ by $k_1 \leftrightarrow -k_2$, or simply

$$U \rightarrow S, \quad F \rightarrow F' \equiv (k_1-q)^2-\mu^2=q^2-2k_1\cdot q. \tag{2.11}$$

The quantity F' is the muon propagator denominator in reaction (1.3).

III. PHASE-SPACE INTEGRATION

The usual procedure[25] (making use of Lorentz invariance) is to analytically integrate first over the final boson-lepton pair in their c.m. frame. This leaves us finally with an over-all two-dimensional numerical integration.

In detail, for the proton target, consider the frame where $\mathbf{k}_1-\mathbf{q}=0$ for a given $\mathbf{p}_2$. Then the argument of the energy δ function is independent of the angles $\mathbf{k}_2$ and $\mathbf{k}$, and we obtain

$$d^3\sigma=\frac{1}{32\pi^3}\frac{\alpha^2 g_W{}^2}{E_1 M_p}\frac{d^3\mathbf{p}_2}{E_{p_2}}\left[\frac{|\mathbf{k}|}{E_2+E_k}\times\int d\Omega_k \mathfrak{F}(T,U,F,B,N)\right]_{\mathbf{k}_1-\mathbf{q}=0 \text{ frame}}. \tag{3.1}$$

All of the arguments of $\mathfrak{F}$, save T, depend on the W's angular orientation and, to make the dependence explicit, we use rotational invariance and choose $\mathbf{k}_1$ along a z axis and $\mathbf{p}$ in the corresponding x-z plane; the angles of W are defined according to the axes shown in Fig. 2. Further details of the integration over Ω_k are given in the Appendix. Besides S and T, the remaining independent has been chosen to be

$$S' \equiv (k+k_2)^2=T-B-F, \tag{3.2}$$

the energy squared of the $W\mu$ duo in their c.m. frame.

Thus the results of the $\mathbf{k}_2$ and $\mathbf{k}$ integrations can be given explicitly and transformed in the manner described in the Appendix to the laboratory frame ($\mathbf{p}_1=0$). Here, we can make use of the azimuthal symmetry about the beam direction and, orienting the z axis for the $\mathbf{p}_2$ integration along this direction, the ϕ_{p_2} part merely yields a factor of 2π.

[25] See, for example, Refs. 4, 5, and 7.

The remaining integration variables E_{p_2} and θ_{p_2} (with respect to $\mathbf{k}_1$) are changed into T and S'; this change, essentially that made by von Gehlen[4] and by Berends and West,[7] is convenient in view of the presence of our form factors. So we now calculate the Jacobian according to

$$E_{p_2}=M_p-T/2M_p, \qquad \cos\theta_{p_2}=\frac{S'-T(1+E_1/M_p)}{2E_1|\mathbf{p}_2|}. \tag{3.3}$$

We have

$$d^2\sigma=\frac{1}{32\pi}\left(\frac{\alpha g_W}{E_1 M_p}\right)^2 d|T|\,dS'\frac{[(S'-1-\mu^2)^2-4\mu^2]^{1/2}}{S'}\times\mathcal{G}_\nu(S,T,S'), \tag{3.4}$$

$$\mathcal{G}_\nu \equiv \frac{1}{4\pi}\left[\int d\Omega_k \mathfrak{F}\right]_{\mathbf{k}_1-\mathbf{q}=0}.$$

The T and S' integrations are handled most simply—and as accurately as necessary—numerically: We employ a Gaussian quadrature routine. For a given allowed value of $T<0$, the minimum value of S' is when the muon and boson are at rest in their c.m. system. The maximum value corresponds to the final proton going forward in the laboratory for fixed values of T. Then

$$S'_{\max}=2E_1|\mathbf{p}_2|+T(1+E_1/M_p), \qquad S'_{\min}=(1+\mu)^2. \tag{3.5}$$

We see that $S'_{\min}$ checks with the zero in the phase-space radical of Eq. (3.4). Equation (3.5) tells us directly how to find the allowed T range, since the maximum value of S' falls below $S'_{\min}$ if $|T|$ is either too large or too small. Therefore

$$\left\{\begin{matrix}|T|_{\max}\\ |T|_{\min}\end{matrix}\right\}=\frac{b\pm(b^2-4ac)^{1/2}}{2a}, \tag{3.6}$$

$$a=S/M_p{}^2, \quad b=4E_1{}^2-2S'_{\min}(1+E_1/M_p), \quad c=S'_{\min}{}^2.$$

The limits in Eq. (3.6) correspond to the vanishing of the S' phase space; alternatively, the maximum arises from the kinematical situation where the proton is going forward (along the beam direction) in the over-all c.m. system and the boson and muon are going backwards together. (They would be at rest in their c.m. frame.) The minimum is when the proton goes backward and the forward-going boson and muon again have the same velocity in the over-all c.m. system. This last case still corresponds to the proton going forward in the laboratory since it cannot be left at rest there (let alone go backward) for nonzero M_W and μ.

Finally we note as a check that the vanishing of the T phase space, i.e., the vanishing of the square root in Eq. (3.6) occurs at the threshold value of E_1 for the W

production:

$$E_1|_{\text{threshold}}=\frac{(M_W+M_p+\mu)^2-M_p^2}{2M_p}. \quad (3.7)$$

The phase-space discussion and formulas necessary for the neutron or infinite-mass target go through in the same manner. We may now give the numerical results.

IV. RESULTS FOR TOTAL CROSS SECTIONS

Implicit in our form factor and kinematics discussion is the fact that we have not allowed for the possibility of target "breakup." In the proton case, it is possible to consider this by using the recent deeply inelastic SLAC and DESY measurements,[26] while in the nuclear case the problem is much more complex. Here, however, we shall just give results for the scattering of a neutrino off of a free nucleon target and for the "coherent" scattering off of several nuclei tragets, both with no new final states due to breakup. Later on in Sec. V we will discuss the mixing of the coherent and incoherent modes, hadron inelasticity, and other nuclear effects.

A. Nucleon Targets

Here we assume the target is a free proton or neutron with mass M_p or M_n, respectively. A W boson can be produced from a neutrino collision off of these targets provided E_1 is larger than the threshold value given by Eq. (3.7).

The form factors are approximated by the dipole fit and scaling law

$$G_E(\text{proton})\cong\frac{G_M(\text{proton})}{2.79}\cong-\frac{G_M(\text{neutron})}{1.91}\cong\left(1-\frac{T}{[0.71\ (\text{GeV}/c)^2]}\right)^{-2}, \quad (4.1)$$

$$G_E(\text{neutron})\cong 0,$$

according to the most recent data.[27] In order to make comparisons with previous work, we have also employed a number of different form-factor fits.

The numerical integration of Eq. (3.4) over the limits given in Eq. (3.6) is shown as an allowed T region (as a function of E_1) in Fig. 3 for the representative masses $M_W=5$ and 8. For large $E_1\gg M_W$, $M_{p,n}$ the maximum value of $|T|$ [cf. Eq. (3.6)] is asymptotically linear in the neutrino energy

$$|T|_{\max}\xrightarrow[E_1\to\infty]{}2M_{p,n}E_1, \quad (4.2)$$

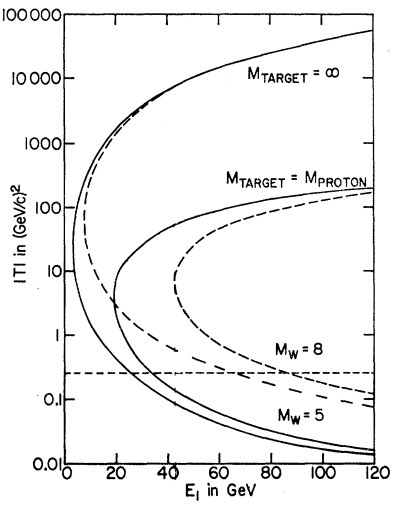

FIG. 3. Momentum transfer in $(\text{GeV}/c)^2$ versus the incident beam energy in GeV. The solid curves are for $M_W=5$ GeV/c^2 and the dashed curves are for $M_W=8$ GeV/c^2. The line at $|T|=0.25$ $(\text{GeV}/c)^2$ represents the cutoff on the nuclear Fermi distribution.

reminiscent of elastic lepton-nucleon scattering. (Recall that here the boson and muon go off together backward in the c.m. system as if they were one particle of negligible mass.) The corresponding asymptotic minimum value is inversely proportional to E_1^2,

$$|T|_{\min}\xrightarrow[E_1\to\infty]{}\frac{S'_{\min}{}^2}{4E_1{}^2}\cong\left(\frac{M_W{}^2}{2E_1}\right)^2. \quad (4.3)$$

The independence of this result of the target mass is related to the fact that any target can be left at rest at extreme energies offering the minimum momentum transfer case. (The boson and muon go off together *forward* in the c.m. system.)

While the larger values of momentum transfer will not contribute much to the cross sections (since the form factors suppress these regions), it is interesting that the smaller values for larger E_1 according to Eq. (4.3) do not correspond to contributions as large as one might expect. This is because of an important cancellation for small T due essentially to gauge invariance. (This was stressed recently in the e^+e^- calculation of Berends and West.[7]) We show here explicitly how this comes about.

After the $\mathbf{k}_2$ and $\mathbf{k}$ integrations, the most general kinematic singularity- and zero-free invariant amplitude expansion deriving from $K_{\beta\alpha}L^{\beta\nu\mu\alpha}$ is[28]

$$(Tg^{\nu\mu}-q^\nu q^\mu)A(T,S')+[Tk_1{}^\nu k_1{}^\mu-k_1\cdot q(k_1{}^\nu q^\mu+q^\nu k_1{}^\mu)+(k_1\cdot q)^2 g^{\nu\mu}]B(T,S'). \quad (4.4)$$

If this gauge-invariant rank-two tensor is contracted into $P_{\nu\mu}$, we obtain for a proton target

$$-G_2S'^2M_p{}^2B(T,S')+(\text{terms with an explicit factor of } T). \quad (4.5)$$

[26] E. D. Bloom *et al.*, Phys. Rev. Letters **23**, 930 (1969); M. Breidenbach *et al.*, *ibid.* **23**, 935 (1969); W. Albrecht *et al.*, Nucl. Phys. **B13**, 1 (1969); B. D. Dieterle *et al.*, Phys. Rev. Letters **23**, 1187 (1969); M. L. Perl *et al.*, *ibid.* **23**, 1191 (1969).

[27] D. H. Coward *et al.*, Phys. Rev. Letters **20**, 292 (1968); J. Litt *et al.*, Phys. Letters **31B**, 40 (1970); W. Bartel *et al.*, *ibid.* **30B**, 285 (1969).

[28] W. N. Cottingham, Ann. Phys. (N. Y.) **25**, 424 (1963).

TABLE I. Theoretical total cross sections σ_ν [reaction (1.1)] and σ_μ [reaction (1.3)] for $M_W=5$ GeV/c^2 in units of 10^{-38} cm^2. $\sigma(p)$, $\sigma(n)$ denote the cross section for scattering off of protons and neutrons with a dipole form factor. $\sigma'(p)$ and $\sigma'(n)$ denote the corresponding cross sections with the exclusion principle and Fermi motion included. σ_{inel} denotes the inelastic cross section discussed in Sec. V A. σ_c(Ne)/10, σ_c(Fe)/26, and σ_c(U)/92 denote the coherent cross sections per proton from neon, iron, and uranium nuclei with Fermi form factors. The total cross section can be calculated by combining these numbers according to Eqs. (5.12) or (5.13).

	$M_W=5$ GeV/c^2											
	ν			μ			ν			μ		
κ	-1	0	$+1$	-1	0	$+1$	-1	0	$+1$	-1	0	$+1$
	$E_l=30$ GeV						$E_l=50$ GeV					
$\sigma(p)$	0.164	0.185	0.210	2.07×10^{-3}	0.723×10^{-3}	1.67×10^{-3}	2.71	3.05	3.50	0.0451	0.0152	0.0428
$\sigma(n)$	0.0667	0.0760	0.0872	9.26×10^{-4}	3.22×10^{-4}	7.47×10^{-4}	0.860	0.989	1.16	0.0179	0.00605	0.0172
$\sigma'(p)$	0.268	0.302	0.343	3.54×10^{-3}	1.22×10^{-3}	2.98×10^{-3}	3.08	3.46	3.98	0.0540	0.0184	0.0524
$\sigma'(n)$	0.103	0.118	0.136	1.55×10^{-3}	0.530×10^{-3}	1.30×10^{-3}	0.934	1.08	1.27	0.0209	0.00712	0.0206
σ_{inel}	0.0298	0.0369	0.0461	9.82×10^{-4}	3.51×10^{-4}	7.84×10^{-4}	0.868	1.08	1.37	0.0359	0.0123	0.0341
σ_c(Ne)/10	8.13×10^{-7}	8.25×10^{-7}	8.38×10^{-7}	8.60×10^{-10}	3.70×10^{-10}	6.37×10^{-10}	4.98×10^{-3}	5.21×10^{-3}	5.48×10^{-3}	1.73×10^{-5}	0.613×10^{-5}	1.39×10^{-5}
σ_c(Fe)/26	3.19×10^{-6}	3.24×10^{-6}	3.30×10^{-6}	3.35×10^{-9}	1.41×10^{-9}	2.48×10^{-9}	3.49×10^{-3}	3.63×10^{-3}	3.79×10^{-3}	1.04×10^{-5}	0.370×10^{-5}	0.843×10^{-5}
σ_c(U)/92	2.53×10^{-6}	2.57×10^{-6}	2.61×10^{-6}	2.60×10^{-9}	1.09×10^{-9}	1.92×10^{-9}	1.95×10^{-3}	2.03×10^{-3}	2.13×10^{-3}	0.624×10^{-5}	0.222×10^{-5}	0.502×10^{-5}
	$E_l=80$ GeV						$E_l=100$ GeV					
$\sigma(p)$	10.1	11.4	13.3	0.235	0.0824	0.249	15.9	18.0	21.2	0.430	0.155	0.474
$\sigma(n)$	2.37	2.76	3.37	0.0799	0.0284	0.0871	3.20	3.74	4.66	0.135	0.0497	0.153
$\sigma'(p)$	9.18	10.4	12.2	0.228	0.0802	0.244	13.7	15.5	18.5	0.409	0.148	0.455
$\sigma'(n)$	2.18	2.55	3.14	0.0779	0.0277	0.0853	2.85	3.36	4.22	0.130	0.0480	0.148
σ_{inel}	4.23	5.23	6.86	0.229	0.0821	0.245	7.21	8.91	11.8	0.447	0.165	0.498
σ_c(Ne)/10	0.171	0.178	0.187	5.93×10^{-4}	2.08×10^{-4}	5.04×10^{-4}	1.08	1.13	1.19	4.01×10^{-3}	1.40×10^{-3}	3.36×10^{-3}
σ_c(Fe)/26	0.103	0.109	0.117	5.84×10^{-4}	1.99×10^{-4}	5.06×10^{-4}	0.432	0.456	0.485	2.23×10^{-3}	0.766×10^{-3}	2.00×10^{-3}
σ_c(U)/92	0.0716	0.0753	0.0796	3.17×10^{-4}	1.10×10^{-4}	2.73×10^{-4}	0.363	0.382	0.405	1.62×10^{-3}	0.562×10^{-3}	1.40×10^{-3}
	$E_l=200$ GeV						$E_l=400$ GeV					
$\sigma(p)$	44.9	50.6	61.5	1.89	0.746	2.22	92.2	103	129	5.74	2.41	6.76
$\sigma(n)$	5.89	6.81	8.99	0.454	0.188	0.548	8.65	9.58	13.3	1.08	0.476	1.26
$\sigma'(p)$	32.3	36.8	45.8	1.66	0.662	1.97	55.9	62.8	81.5	4.58	1.96	5.42
$\sigma'(n)$	4.96	5.76	7.71	0.421	0.176	0.510	7.15	7.88	11.1	0.971	0.432	1.14
σ_{inel}	23.9	29.0	40.2	2.23	0.902	2.67	54.4	63.3	91.9	7.29	3.10	8.83
σ_c(Ne)/10	29.8	32.0	34.7	0.257	0.0875	0.244	160	176	198	2.83	1.01	3.05
σ_c(Fe)/26	33.4	35.4	38.2	0.218	0.0744	0.198	268	292	325	3.74	1.30	3.88
σ_c(U)/92	14.7	15.6	16.6	0.0809	0.0281	0.0743	341	366	398	3.15	1.08	3.04
	$E_l=600$ GeV						$E_l=1000$ GeV					
$\sigma(p)$	129	143	182	9.83	4.22	11.4	186	202	262	17.8	7.78	20.1
$\sigma(n)$	10.4	11.0	15.7	1.61	0.725	1.82	12.7	12.7	18.5	2.50	1.13	2.65
$\sigma'(p)$	71.4	78.5	105	7.40	3.25	8.56	92.6	98.5	135	12.5	5.55	13.8
$\sigma'(n)$	8.54	9.00	13.0	1.45	0.650	1.62	10.5	10.3	15.2	2.20	0.993	2.31
σ_{inel}	80.2	89.8	134	18.8	8.03	22.1	123	130	200	24.5	10.4	28.4
σ_c(Ne)/10	308	340	394	7.70	2.88	8.71	579	643	765	21.3	84.3	24.9
σ_c(Fe)/26	574	631	720	11.7	4.26	12.9	1180	1310	1534	36.3	14.0	42.0
σ_c(U)/92	972	1061	1183	13.7	4.77	14.2	2460	2710	3110	55.1	20.3	61.5

Therefore the leading terms must conspire to cancel partially for small momentum transfers and any mass target. Notice that the small-T limit corresponds to the vanishing of phase space and the phase-space factor and further note that $\mathcal{G}_\nu$ of Eq. (3.4) is $O(\mu^2)$ in that limit [owing to the $(k_2+\mu)$ factor in (2.8)].

The aforementioned role of current conservation is especially crucial in electron-positron colliding beams since there M_p is replaced in (4.5) by the electron mass. In particular, a calculation in the literature[29] of the reaction

$$e^+ + e^- \rightarrow e^+ + W^- + \nu_e$$

was incorrect by a factor of a million simply because gauge invariance was not maintained; there then appeared an anomalous linear divergence in the electron mass squared. Berends and West[7] have since calculated this more carefully obtaining the correct cancellation. As a check of our programs it was not hard to convert our situation to the e^+e^- c.m. case and good agreement with their results was achieved.

In spite of this cancellation, the small-T region is still the most important and the numerical integration has to be done carefully over this region. Bearing this in mind, we have calculated the total cross sections σ_ν for an assorted array of energies, boson masses and anomalous magnetic moments. The σ_ν values for E_1 between 30 and 1000 GeV, $M_W=5$, 10, and 15 GeV/c^2, and $\kappa=0, \pm 1$[30] are listed in Tables I–III for the proton.[31] These tables also illustrate the neutron case. To get a better idea of the σ_ν energy dependence, the proton and neutron results are plotted in Fig. 4 for $\kappa=0, \pm 1$ and $M_W=7$ GeV/c^2. Also, Fig. 5 shows $d\sigma/d|T|$ for both proton and neutron at $E_1=50$ GeV, $M_W=5$ GeV/c^2, and $\kappa=0$.

We see that if the beam luminosities will allow the measurement of cross sections on the order of 10^{-38} cm^2, a proton will be an adequate target for upwards of 10-GeV bosons provided that 100-GeV neutrinos are available. It should be noted that the unit variation in κ changes the results very little and even the most pronounced variations, which occur at large energies and small M_W, are never as much as 50%. The neutron cross sections are consistently a factor of 2–10 smaller for the range of energies and masses in our tables.

In order to check our numerical work, we have calculated σ_ν(nucleon) for several configurations of masses and energies that were also considered by Wu *et al.*[5] When we used their form factors remarkable agreement for every combination was reached (within 1%). The difference wrought by changing to the dipole fit (4.1) was only a few percent. The computations relating to the input considered by Lee *et al.*[1] were also performed

TABLE II. Same as Table I with $M_W=10$ GeV/c^2.

	ν			μ			ν			μ		
κ	-1	0	$+1$	-1	0	$+1$	-1	0	$+1$	-1	0	$+1$
				$E_1=100$ GeV					$E_1=200$ GeV			
$\sigma(p)$	0.0923	0.0991	0.107	4.69×10^{-4}	1.68×10^{-4}	3.63×10^{-4}	4.37	4.76	5.26	0.0471	0.0159	0.0449
$\sigma(n)$	0.0405	0.0436	0.0471	2.16×10^{-4}	0.771×10^{-4}	1.67×10^{-4}	1.41	1.55	1.74	0.0187	0.00633	0.0181
$\sigma'(p)$	0.175	0.188	0.204	1.02×10^{-3}	0.358×10^{-3}	0.827×10^{-3}	4.85	5.28	5.86	0.0561	0.0191	0.0546
$\sigma'(n)$	0.0790	0.0790	0.0858	4.60×10^{-4}	1.61×10^{-4}	3.73×10^{-4}	1.50	1.66	1.87	0.0218	0.0074	0.0215
σ_{inel}	0.0387	0.0445	0.0514	5.87×10^{-4}	2.07×10^{-4}	4.57×10^{-4}	2.29	2.68	3.25	0.0643	0.0220	0.0625
σ_e(Ne)/10							7.41×10^{-3}	7.67×10^{-3}	7.97×10^{-3}	1.76×10^{-5}	0.620×10^{-5}	1.40×10^{-5}
σ_e(Fe)/26							6.64×10^{-3}	6.90×10^{-3}	7.21×10^{-3}	1.06×10^{-5}	0.374×10^{-5}	0.852×10^{-5}
σ_e(U)/92							3.15×10^{-3}	3.25×10^{-3}	3.36×10^{-3}	0.636×10^{-5}	0.225×10^{-5}	0.509×10^{-5}
				$E_1=400$ GeV					$E_1=1000$ GeV			
$\sigma(p)$	21.8	23.9	27.3	0.435	0.157	0.479	74.0	81.4	96.4	2.79	1.13	3.29
$\sigma(n)$	4.38	4.94	5.88	0.136	0.0502	0.155	8.45	9.44	12.1	0.619	0.263	0.745
$\sigma'(p)$	18.7	20.6	23.7	0.414	0.150	0.459	50.0	55.4	67.3	2.38	0.975	2.83
$\sigma'(n)$	3.90	4.42	5.30	0.131	0.0485	0.150	7.05	7.89	10.3	0.568	0.244	0.686
σ_{inel}	13.5	16.0	20.2	0.641	0.238	0.719	50.6	59.0	79.6	4.38	1.81	5.27
σ_e(Ne)/10	1.61	1.67	1.73	4.02×10^{-3}	1.41×10^{-3}	3.36×10^{-3}	75.8	80.5	86.8	0.631	0.216	0.627
σ_e(Fe)/26	0.664	0.690	0.721	2.24×10^{-3}	0.767×10^{-3}	2.00×10^{-3}	103	109	116	0.643	0.219	0.609
σ_e(U)/92	0.528	0.548	0.572	1.63×10^{-3}	0.563×10^{-3}	1.40×10^{-3}	75.0	78.5	82.3	0.306	0.106	0.278

[29] E. A. Choban, Yadern. Fiz. **7**, 375 (1968) [Soviet J. Nucl. Phys. **7**, 245 (1968)].

[30] Since the cross section is quadratic in κ, these three cases suffice to determine the κ dependence everywhere.

[31] Other numbers are available upon request.

TABLE III. Same as Table I with $M_W=15$ GeV/c^2.

	$M_W=15$ GeV/c^2											
	ν			μ			ν			μ		
κ	-1	0	$+1$	-1	0	$+1$	-1	0	$+1$	-1	0	$+1$
			$E_1=200$ GeV						$E_1=400$ GeV			
$\sigma(p)$	0.0420	0.0443	0.0467	1.23×10^{-4}	0.449×10^{-4}	0.921×10^{-4}	3.67	3.93	4.25	0.0282	0.00952	0.0260
$\sigma(n)$	0.0191	0.0201	0.0212	5.73×10^{-5}	2.09×10^{-5}	4.31×10^{-5}	1.27	1.37	1.51	0.0116	0.00390	0.0108
$\sigma'(p)$	0.0996	0.105	0.111	3.61×10^{-4}	1.28×10^{-4}	2.84×10^{-4}	4.13	4.43	4.81	0.0348	0.0118	0.0328
$\sigma'(n)$	0.0431	0.0457	0.0485	1.65×10^{-4}	0.584×10^{-4}	1.30×10^{-4}	1.38	1.49	1.64	0.0139	0.0047	0.0133
σ_{inel}	0.0284	0.0315	0.0352	2.67×10^{-4}	0.962×10^{-4}	2.02×10^{-4}	2.31	2.64	3.10	0.0490	0.0166	0.0465
σ_c(Ne)/10							4.18×10^{-3}	4.28×10^{-3}	4.40×10^{-3}	5.39×10^{-6}	1.95×10^{-6}	4.13×10^{-6}
σ_c(Fe)/26							2.01×10^{-3}	2.06×10^{-3}	2.12×10^{-3}	3.33×10^{-6}	1.18×10^{-6}	2.64×10^{-6}
σ_c(U)/92							1.40×10^{-3}	1.43×10^{-3}	1.47×10^{-3}	1.99×10^{-6}	0.711×10^{-6}	1.55×10^{-6}
			$E_1=600$ GeV						$E_1=1000$ GeV			
$\sigma(p)$	11.4	12.3	13.6	0.137	0.0471	0.140	30.0	32.6	36.7	0.563	0.206	0.629
$\sigma(n)$	3.06	3.36	3.79	0.0498	0.0172	0.0521	5.59	6.22	7.33	0.170	0.0637	0.196
$\sigma'(p)$	10.7	11.6	12.8	0.135	0.0464	0.138	25.0	27.3	31.0	0.530	0.195	0.598
$\sigma'(n)$	2.88	3.16	3.59	0.0490	0.0170	0.0514	4.92	5.50	6.54	0.162	0.0612	0.189
σ_{inel}	7.76	8.98	10.8	0.235	0.0825	0.246	21.7	25.3	31.5	0.980	0.369	1.12
σ_c(Ne)/10	5.71×10^{-2}	5.89×10^{-2}	6.10×10^{-2}	1.40×10^{-4}	0.479×10^{-4}	1.21×10^{-4}	3.76	3.88	4.03	9.07×10^{-3}	3.15×10^{-3}	7.66×10^{-3}
σ_c(Fe)/26	0.754×10^{-3}	0.778×10^{-3}	0.806×10^{-2}	1.67×10^{-4}	0.584×10^{-4}	1.38×10^{-4}	1.89	1.95	2.02	4.56×10^{-3}	1.58×10^{-3}	4.04×10^{-3}
σ_c(U)/92	0.366×10^{-2}	0.378×10^{-2}	0.391×10^{-2}	0.846×10^{-4}	0.294×10^{-4}	0.702×10^{-4}	1.02	1.06	1.11	3.26×10^{-3}	1.12×10^{-3}	2.85×10^{-3}

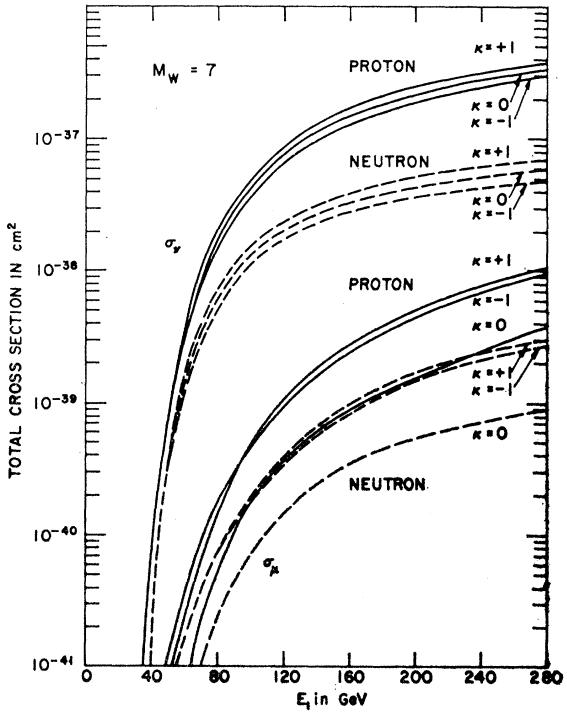

FIG. 4. Neutrino and muon total cross sections off of protons and neutrons with dipole form factors $M_W=7$ GeV/c^2 and $\kappa=0,\pm1$.

and good agreement (using the form factors of that paper) was reached as well.

Some other higher-energy results tabulated recently[15] are apparently incorrect. Even when we use the same form factors that Berkov *et al.* employ, we find that our values are consistently about a factor of 6–10 smaller than theirs for all of the cases that they considered—nuclei and nucleon targets.

B. Nuclei Targets

For a first approximation of coherent scattering, we treat the nuclei cases in the static limit. The target mass M_∞ is taken to be much larger than anything else around and so the beam energy threshold, $M_W+\mu$, is much lower here since the target acquires negligible energy. As we shall see, however, the nuclei form factors drastically reduce the coherent cross sections unless we are far above threshold anyway.

The electromagnetic form factor employed corresponds to the Fermi nuclear charge density[32]

$$\rho_f(r)=C/(1+e^{(r-R)/b}),$$
$$R=1.07A^{1/3}\times10^{-13}\text{ cm},\qquad(4.6)$$
$$b=0.568\times10^{-13}\text{ cm},$$

where A is the atomic number and C is determined by $\int\rho_f(r)d^3r=Z$ with Z the total charge of the nucleus.

[32] R. Herman and R. Hofstadter, *High Energy Electron Scattering Tables* (Stanford U. P., 1960). See also Ref. 3.

Specifically, the form factor is

$$F_f(\mathbf{q}^2)=4\pi\theta(500\text{ MeV}/c-|\mathbf{q}|)\int_0^\infty r^2dr \times\rho_f(r)\frac{\sin(|\mathbf{q}|r)}{|\mathbf{q}|r}, \tag{4.7}$$

where, as an added condition, the region $|T|>0.25$ $(\text{GeV}/c)^2$ has been cut off.[3] (Of course, $T=-\mathbf{q}^2=-\mathbf{p}_2^2$ in the static case.) This distribution adds an extra integration to our computer program. In checking our programs with previous results, we have had occasion to also employ the exponential density[1]

$$\rho_e(r)=\rho_e(0)e^{-(\sqrt{12})r/a}, \quad a=(\sqrt{\tfrac{3}{5}})\times(1.3A^{1/3})\times10^{-13}\text{ cm}, \tag{4.8}$$

which in turn leads to the familiar dipole form factor

$$F_e(\mathbf{q}^2)=\frac{Z}{(1+\mathbf{q}^2a^2/12)^2}. \tag{4.9}$$

Generally larger than (4.7), this also serves an upper bound as well. Since the proton trace (2.6) is

$$4M_p^2[G_E^2(T)\delta_{\mu0}\delta_{\nu0}+O(1/M_p)],$$

in practice we have just substituted our nuclei form factors for G_E and G_M, using some large mass target (say 10 000 GeV) in our numerical work. In this way we would simply convert the nucleon calculation to the nuclei case and also, by reducing this target mass, check the recoil effects on a spin-zero target (which were small). A plot of $|F_f|$ for the two nuclei, neon and uranium, is given along with the proton electric form factor G_E in Fig. 6.

As in the nucleon target discussion, the T limits as a function of E_1 are plotted in Fig. 3 for the M_∞ case according to the M_∞ limit of Eq. (3.6):

$$\left\{\begin{matrix}|T|_{\max}\\|T|_{\min}\end{matrix}\right\}=2E_1^2[1-S'_{\min}/2E_1^2 \pm(1-S'_{\min}/E_1^2)^{1/2}]. \tag{4.10}$$

Therefore,

$$\left\{\begin{matrix}|T|_{\max}\\|T|_{\min}\end{matrix}\right\}\xrightarrow[E_1\to\infty]{}\left\{\begin{matrix}4E_1^2\\(S'_{\min}/2E_1)^2\cong(M_W^2/2E_1)^2.\end{matrix}\right. \tag{4.11}$$

These asymptotic values can be compared to Eqs. (4.2) and (4.3); this comparison and Fig. 3 together show the expected result. A static source can absorb larger momentum transfers than the nucleon can but their minimum values are the same for high energies.

The previous nucleon discussion concerning the important regions of the T integration apply here as well—especially since we truncate the Fermi form factor $\mathbf{q}^2>0.25$ $(\text{GeV}/c)^2$. A plot of $d\sigma_c/d|T|$ for an iron target is shown in Fig. 5 for $M_W=5$, $\kappa=0$, and $E=50$.

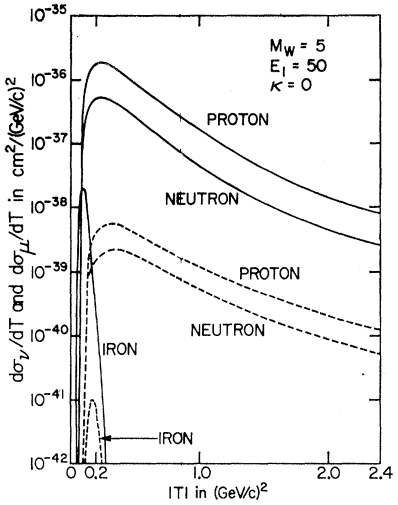

FIG. 5. $d\sigma_\nu/d|T|$ (solid lines) and $d\sigma_\mu/d|T|$ (dashed lines) versus $|T|$ in $(\text{GeV}/c)^2$ for scattering on protons and neutrons (with dipole form factors) and iron (with Fermi form factors). Here, $M_W=5$ GeV/c^2, $E_l=50$ GeV, $\kappa=0$.

We have calculated the coherent cross section σ_c over the same energies and masses considered in the nucleon-target configuration. Even though the threshold for a given W can be much lower in the coherent case, the resulting minimum momentum transfer is so large for the lower energies that the nuclei form factors suppress the cross section below any observable value (cf. Fig. 5). Some various nuclei target results for neon, iron, and uranium are listed in Tables I, II, and III, respectively. More results are plotted in Figs. 7 and 8 at the typical masses $M_W=3$ and 8, respectively, for $\kappa=0$.

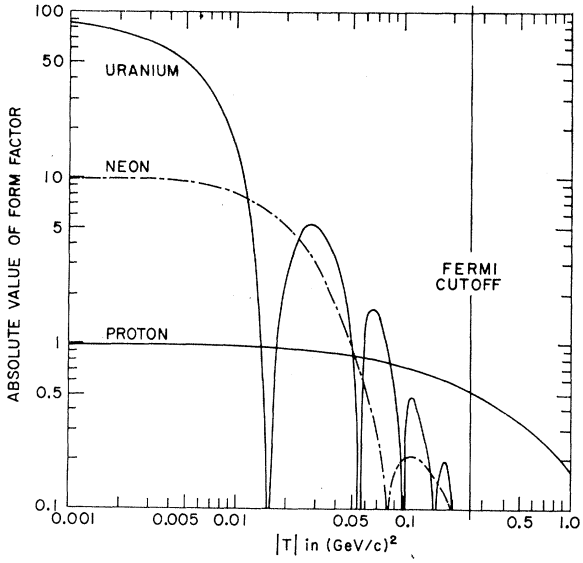

FIG. 6. Nuclear Fermi form factors and the proton dipole form factor versus $|T|$. The solid line is for uranium and the dashed line for neon.

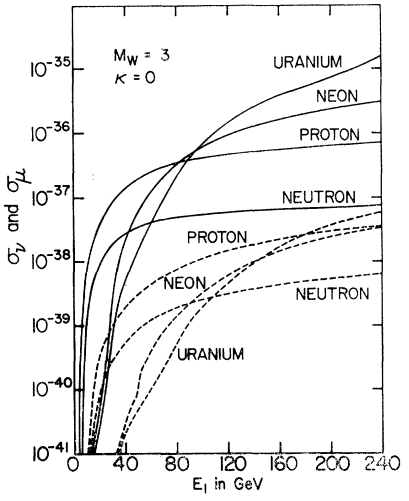

FIG. 7. Incoherent total cross sections (in cm²) off of protons and neutrons and coherent total cross sections (per proton) off of neon and uranium for the mass $M_W=3$ GeV/c^2 and $\kappa=0$. The solid lines are for the neutrino-induced reaction and the dashed lines are for the muon-induced reaction.

The coherent results are not surprising. For a given mass M_W, we need to go to very large energies before the factor of Z in the cross section *per proton* overcomes the rapid falloff of the Fermi form factor enough to be comparable with the individual proton scattering. Note that the coherent form factors, especially for larger A, drop off much faster than those for individual nucleons and thus the over-all Z^2 does not come into play until sufficiently small momentum transfers are available. It is also interesting to note that the increase in nuclear spatial extension for larger A produces more oscillations in the Fermi form factor (4.7) as seen in Fig. 6. This in turn produces some bumps in σ_ν visible in Figs. 7 and 8.

Again, we have checked our results against Wu *et al.*[5] and obtained nice agreement with their published data for nuclei. Also it should be stated that using the dipole fit (4.10), we found good agreement (within 5%) with the results of Lee *et al.*[1]

V. INELASTICITY AND NUCLEAR EFFECTS

The coherent and incoherent cases represent idealized extremes and in reality we shall be dealing with more complicated situations when we talk about an actual experiment. Even for hydrogen targets, the problem of inelastic channels comes to light in view of the recent data[26] from deep-inelastic electron-proton scattering. In scattering from nuclei, besides a complicated inelastic channel possibility, there is the nucleon-nucleon interaction which leads to something between an incoherent constituent scattering and a tightly bound coherent collision. We cannot pretend to treat these things carefully but an attempt will be made to categorize and crudely estimate these effects.

A part of our effort will be to take other calculations in the literature concerning the effects of interest and apply their approaches here. The important questions to be answered are (1) whether the nuclear distribution complications will reduce our incoherent cross sections below a visible level, and (2) whether the inelastic channel contributions will overwhelm our elastic results.

In Sec. V A, we address ourselves to the inelastic channels available for hydrogen targets. Section V B covers the case of nuclei: target recoil, nucleon motion, and the exclusion principle.

A. Proton Target

In scattering from hydrogen targets, the individual hadron inelastic channels (e.g., formation of resonances at the photon-proton vertex) can, in principle, be taken into account. However, we expect the resonance form factors to drop off as fast as the nucleon ones[33]; this expectation coupled with the larger minimum momentum transfers and higher-energy thresholds leads us to believe that the resonance contributions will always be quite a bit smaller than our nucleon ones. One main source of worry, however, is that the deep-inelastic form factors do not fall off so fast and might give a large contribution. This contribution to the neutrino-induced reaction has already been treated by two authors,[16,17] but not with the same result. Chen[16] finds it is always smaller than that for the single-proton final state and Folomeshkin[17] states that this contribution is an order of magnitude *larger*. In view of this serious disagreement it is important to have another evaluation.

Therefore we now reconsider an estimate of this inelastic process which presumably includes a large number of undetected final hadron states at the nucleon-photon-hadron vertices in Fig. 1. Utilizing the notation of Breidenbach *et al.*,[26] we find, for some $p_2^2=W^2$, that

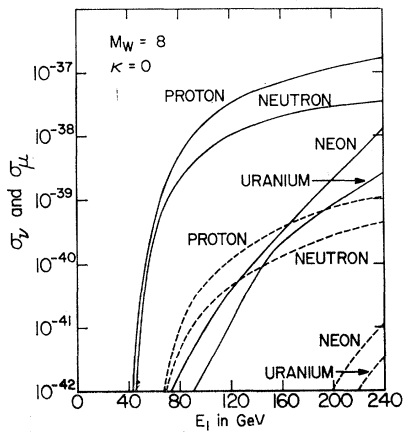

FIG. 8. Same as Fig. 7 but with $M_W=8$ GeV/c^2, $\kappa=0$.

[33] W. W. Ash *et al.*, Phys. Letters **24B**, 165 (1967); W. Bartel *et al.*, *ibid.* **27B**, 660 (1968); W. Albrecht *et al.*, *ibid.* **28B**, 225 (1968); C. Mistretta *et al.*, Phys. Rev. Letters **20**, 1070 (1968); D. Imrie *et al.*, *ibid.* **20**, 1074 (1968).

the analog of Eq. (3.4) is

$$d^3\sigma=\frac{1}{32\pi}\left(\frac{\alpha g_W}{E_1M_p}\right)^2 dW^2d|T|dS'\frac{[(S'-1-\mu^2)^2-4\mu^2]^{1/2}}{S'}\times\mathcal{G}_\nu^{\text{inel}}(S,T,S',W^2), \quad (5.1)$$

where $\mathcal{G}_\nu^{\text{inel}}$ is discussed later and in the Appendix. Except for $S'_{\min}$, the limits of integration are now changed from the proton case given in (3.5) and (3.6). For a given T and W,

$$S'_{\max}=2E_1|\mathbf{q}|+T(1+E_1/M_p)-(E_1/M_p)\Delta,$$
$$S'_{\min}=(1+\mu)^2, \quad (5.2)$$

and for a given W, (3.6) is changed according to

$$a=S/M_p^2,$$
$$b=4E_1^2-2S'_{\min}(1+E_1/M_p)-2(E_1/M_p)\Delta, \quad (5.3)$$
$$c=S'_{\min}(S'_{\min}+2(E_1/M_p)\Delta),$$

with

$$\Delta\equiv W^2-M_p^2, \quad |\mathbf{q}|=(\nu^2-T)^{1/2},$$
$$\nu\equiv q^0=\frac{p_1\cdot q}{M_p}=\frac{1}{2M_p}[\Delta-T]. \quad (5.4)$$

Finally, since W^2 ranges from the single-pion threshold to the maximum value allowed at a given E_1,

$$W_{\max}=(\sqrt{S})-1-\mu,$$
$$W_{\min}=M_p+m_\pi. \quad (5.5)$$

In calculating $\mathcal{G}_\nu^{\text{inel}}$ of Eq. (5.1), the target trace (2.6) now reads, in the language of Drell and co-workers,[34]

$$P_{\nu\mu}^{\text{inel}}=2M_pW_{\nu\mu},$$

where

$$W_{\nu\mu}=-\left(g_{\nu\mu}-\frac{q_\nu q_\mu}{T}\right)W_1(T,\nu)+\frac{1}{M_p^2}\left(p_{1\nu}-\frac{p_1\cdot q}{T}q_\nu\right)\times\left(p_{1\mu}-\frac{p_1\cdot q}{T}q_\mu\right)W_2(T,\nu). \quad (5.6)$$

Assuming scaling (for νW_2) and neglecting the longitudinal photoabsorption cross section,[35] we write

$$\nu W_2(T,\nu)=F(\omega), \quad \omega\equiv-2M_p\nu/T \quad (5.7)$$

and

$$W_1=\left(\frac{\nu^2-T}{-T}\right)\frac{W_2}{1+R}, \quad R\equiv\sigma_l/\sigma_t\cong 0. \quad (5.8)$$

[34] S. Drell and J. D. Walecka, Ann. Phys. (N.Y.) **28**, 18 (1964); S. D. Drell, D. J. Lévy, and T.-M. Yan, Phys. Rev. Letters **22**, 744 (1969).

[35] Scaling, first discussed by Bjorken [J. D. Bjorken, Phys. Rev. **179**, 1547 (1969)], is in agreement with the data accumulated so far (see Ref. 26). The experimental results from DESY [W. Albrecht *et al.*, DESY Report No. 69/46, 1969 (unpublished)] are consistent with $\sigma_l/\sigma_t=0$.

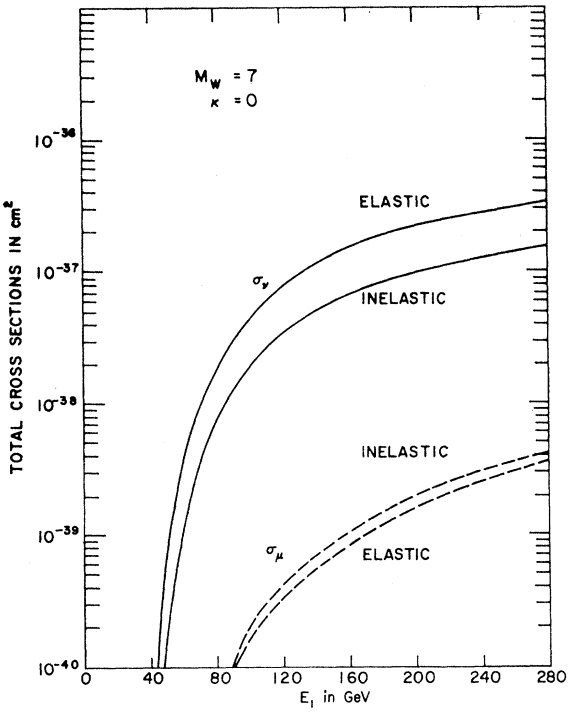

FIG. 9. Total cross sections (in cm²) for scattering off of protons with $M_W=7$ GeV/c^2, $\kappa=0$, dipole form factors compared with the deep-inelastic total cross sections. Again the solid curves represent the neutrino-induced reaction and the dashed curves the muon-induced reaction.

Finally, the crude fit to the data[26] used is

$$F(\omega)\cong 0.4\frac{1-e^{-(\omega-1)}}{1+\omega/20}. \quad (5.9)$$

The factor $(1+\omega/20)^{-1}$ is consistent with the slight drop in the data for large ω and, more importantly, yields the kinematic zero known to be present in νW_2 at $T=0$. It should be emphasized that the calculation here is rather insensitive to the details of the fit (5.9). For example, removing the $(1+\omega/20)^{-1}$ factor increases the cross sections about 20%. If R is changed to, say, 1, we find a 10–20% decrease.

The three integrals over (5.1) are done numerically and it is found that this contribution to the total neutrino cross section is always less than the proton-target contribution. We list the values for this along with the previous numbers in Tables I–III; a curve showing the energy dependence for $M_W=7$ and $\kappa=0$ is plotted in Fig. 9. We therefore agree with Chen; our values are within 20% of his. Using Folomeshkin's fit,[17]

$$F(\omega)\cong 0.3, \quad (5.10)$$

the inelastic cross sections are increased from the values we have presented by a factor of 3 but are not an order of magnitude larger than our proton calculations.

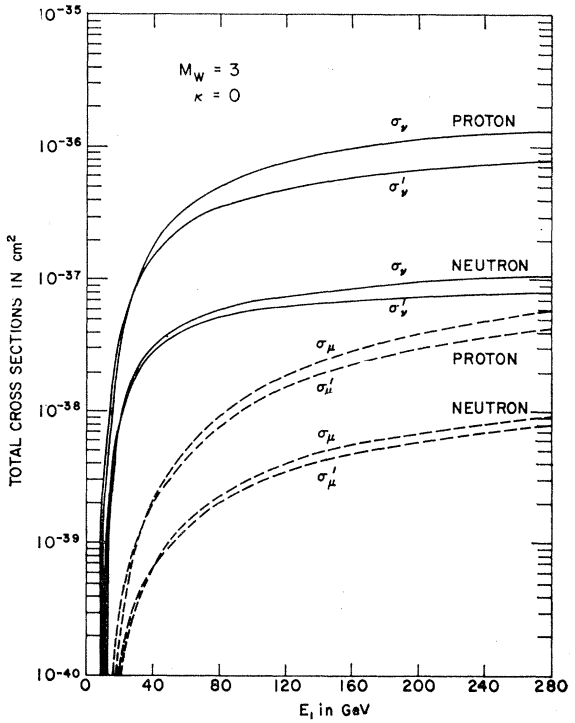

FIG. 10. Effects of the Pauli exclusion principle and the Fermi motion of the nucleons on the proton and neutron total cross sections for $M_W=3$ GeV/c^2 and $\kappa=0$. The solid and dashed lines represent the neutrino and muon results, respectively.

B. Nuclei Targets

Nuclear effects are very complicated and would have to be considered in detail if the W boson is indeed found in future experiments. Here we only give a rough treatment designed to estimate two important effects; nucleon motion and the exclusion principle.

We have a close parallel here to the inelastic scattering of electrons from nuclei. Taking into account only the proton's static charge interaction (the nucleons are treated as massive) and summing over all nuclear states so that closure can be implemented, we can write[36]

$$\frac{d\sigma}{d|\mathbf{q}|^2}=\frac{4\pi\alpha^2}{|\mathbf{q}|^4}[Z+Z(Z-1)f_2(|\mathbf{q}|^2)] \qquad (5.11)$$

if all energy transfers for a given $|\mathbf{q}|^2$ are integrated over. The two-body correlation function f_2 is small for momentum transfers larger than the inverse of the average nucleon separation, implying incoherent addition of the individual proton scatterings. For very small momentum transfers, f_2 approaches unity and we obtain coherent scattering. Inclusion of the N neutrons in the nucleus to first approximation involves an addition only to the incoherent part such that in our case, we could say, in terms of the coherent cross section σ_c,

$$\sigma(\text{total})=Z\sigma_p+N\sigma_n+(1-1/Z)\sigma_c. \qquad (5.12)$$

However, (5.12) is too crude even for us. The Pauli exclusion principle, being a many-body correlation, prohibits small momentum transfers to the individual nucleons and, furthermore, nucleon motion will lower the threshold needed for a given M_W. To investigate these effects on the incoherent cross section, we shall use the Fermi gas model as a framework and incorporate into our programs the exclusion principle effects of Bell and Veltman[3] and the Fermi motion approach of von Gehlen.[4]

We shall combine these two approaches in the following simple fashion. The nucleon motion serves mainly to lower the threshold for a given M_W. So, where the slope of our cross sections is very large as a function of E_1, the cross sections are increased appreciably. On the other hand, we have already seen for large E_1, that the slope becomes more gradual and thus the motion effect is negligible. But it is precisely where this becomes less important that the exclusion principle (which in the gas model suppresses the final nucleon momenta inside the Fermi sphere) begins to play a role—since very small momentum transfers are now realized. As an example, we have plotted the changes in the proton and neutron cross sections due to these two mechanisms for $M_W=3$ and $\kappa=0$ in Fig. 10, and indeed they operate in mutually exclusive regions. (We refer the reader to Refs. 3 and 4 for the details of this computation but it should be noted that we do a four-dimensional integration now for the nucleon-motion effect.) The incoherent results in Figs. 7 and 8 include these effects.

As a result of the noninterference between the two nucleon effects, we have combined them into one correction and call the resulting total cross section σ' in our tables and figures—hence we have not attacked the problem of the motion effect on the exclusion suppression.[37] Listing the values for the same array of masses and energies that were considered in the previous calculations in Tables I–III, we see that the exclusion principle effects a reduction of roughly 50% at high energies for protons and 20% for neutrons. The Fermi motion increases the probability of scattering near threshold by factors of 2 or 3 as expected but only where the cross sections are small to begin with. Also this effect decreases as we increase the incident beam energy. A total cross section including incoherent cross sections would be something like

$$\sigma(\text{total})=Z\sigma_p'+N\sigma_n'+\sigma_c(\text{nucleus}) \qquad (5.13)$$

in the gas model. We have not explicitly listed this combination but merely note that (5.13) is in some sense a refinement over (5.12) and is probably to be preferred.

[36] S. D. Drell, in *Proceedings of the International School of Physics "Ettore Majorana," Erice, Italy, 1969*, edited by A. Zichichi (Academic, New York, to be published); SLAC Report No. SLAC-PUB No. 689 (unpublished). Kinematic refinements can be found in S. D. Drell and C. L. Schwartz, Phys. Rev. **112**, 568 (1958).

[37] In this regard, see the remarks in Ref. 3.

Nuclear recoil effects have been taken into account by varying the "mass" of the nucleus in our coherent calculation. If we take the actual masses rather than a very large mass, we find very little change (less than 1%) in the total cross-section values. This is presumably a result of the fact that the energy transfer is still effectively zero due to the sharp form-factor cutoff [cf. Eq. (3.3)].

One might wish to add the (deep) inelastic calculations in some way to (5.13); here the exclusion-principle effect is difficult to simulate by the lack of identification of the final state. Although the motion of the initial nucleons can be taken into account here in the same way as in the σ' calculation, it involves five integrations and is most simply estimated by analogy with the nucleon case. As a result of recent conjectures,[38] our inelastic calculation is probably a good first approximation for the neutron inelastic cross section as well.

VI. MUON REACTION

We shall parallel our discussion here with what has already been said about the neutrino reaction (1.1). The Feynman diagrams for the muon reaction (1.3) in lowest-order perturbation theory are also included in Fig. 1. Here, k_1 refers to the initial muon and k_2 to the final-state neutrino; then $\mathfrak{F}$ of (2.5) differs from this case by the substitution $k_1 \leftrightarrow -k_2$.

We have in the laboratory

$$d^9\sigma=\frac{1}{2}\frac{1}{32\pi^3}\frac{\alpha^2 g_W{}^2}{|\mathbf{k}_1|M_p}\frac{d^3\mathbf{k}_2}{E_2}\frac{d^3\mathbf{k}}{E_k}\frac{d^3\mathbf{p}_2}{E_{p_2}}\times\delta^4(k_1-q-k_2-k)\mathfrak{F}(T,S,F',B,N),$$
$$S=M_p{}^2+2M_pE_1+\mu^2, \tag{6.1}$$

for an unpolarized muon beam and proton target. We discuss polarized beams later in this section. Relegating a more detailed discussion of $\mathfrak{F}$ to the Appendix, note that we have now chosen T, S, F', B, and N as our independent variables in this section. Moreover, F', defined previously in (2.13), does not depend on the angles of the W in the $W\nu$ c.m. frame:

$$F'=S'-\mu^2. \tag{6.2}$$

This means that the procedure outlined in Sec. III is even better suited for our situation here and, in fact, was the method used in Ref. 7.

We will divide this section into four parts. Section VI A will deal with the nucleon targets and their contribution to the incoherent part of a nuclei cross section, while Sec. VI B is devoted to the coherent calculation. We give the results for the deep-inelastic case in Sec. VI C. Finally the differences between the analogous muon and neutrino cross sections are discussed in Sec. VI D.

Before this presentation, it is expedient to write here the muon limits corresponding to Eqs. (5.2) and (5.3):

$$S'_{\max}=2|\mathbf{k}_1||\mathbf{q}|+T(1+E_1/M_p)-(E_1/M_p)\Delta+\mu^2,\quad S'_{\min}=1 \tag{6.3}$$

and

$$a=S/M_p{}^2,$$
$$b=4|\mathbf{k}_1|^2-2F'_{\min}\left(1+\frac{E_1}{M_p}\right)-2\frac{E_1}{M_p}\Delta-2\frac{\mu^2}{M_p{}^2}\Delta,$$
$$c=F'_{\min}\left(F'_{\min}+2\frac{E_1}{M_p}\Delta\right)+\frac{\mu^2}{M_p{}^2}\Delta. \tag{6.4}$$

One can see that these are identical to (5.2) and (5.3) (note that $F'_{\min}=1-\mu^2$) in the limit $\mu=0$. We could just as well have neglected the muon mass here, but it is convenient to keep the general form for ease in transforming to positron targets in other calculations. Evaluated for the appropriate target and final hadron masses, Eqs. (6.3) and (6.4) fulfill the needs of the cases which follow.

A. Nucleon Targets

The threshold for E_1 is effectively the same here as in Eq. (3.11),

$$E_1|_{\text{threshold}}=\frac{(M_W+M_{p,n})^2-M_{p,n}{}^2-\mu^2}{2M_{p,n}},$$

those changes due to the motion in some nucleus being taken into account as before in von Gehlen's approach. Of course, the phase space is approximately the same in the two reactions since we address ourselves only to ultrarelativistic muon beams. The only difference is one of principle; those limits which heretofore corresponded to the final-state muon at rest in the $W\mu$ c.m. system now are related to the final-state neutrino with zero energy (e.g., $S'_{\min}$). As before,

$$|T|_{\max}\xrightarrow[E_1\to\infty]{}2M_{p,n}E_1,\qquad |T|_{\min}\xrightarrow[E_1\to\infty]{}F'_{\min}{}^2/4E_1{}^2. \tag{6.5}$$

The differential cross section for a proton takes the form here

$$d^2\sigma=\frac{1}{2}\frac{1}{32\pi}\left(\frac{\alpha g_W}{|\mathbf{k}_1|M_p}\right)^2 d|T|\,dS'\frac{S'-1}{S'}\mathcal{G}_\mu(S,T,S'), \tag{6.6}$$

to be compared with (3.4). Notice that $\mathcal{G}_\mu$ is the result of integrating (6.1) over $\mathbf{k}_2$ and $\mathbf{k}$ in the manner described earlier and in the Appendix.

[38] J. D. Bjorken and E. A. Paschos, Phys. Rev. **185**, 1975 (1969); S. D. Drell, D. J. Lévy, and T.-M. Yan, Ref. 34; H. Harari, Phys. Rev. Letters **24**, 286 (1970).

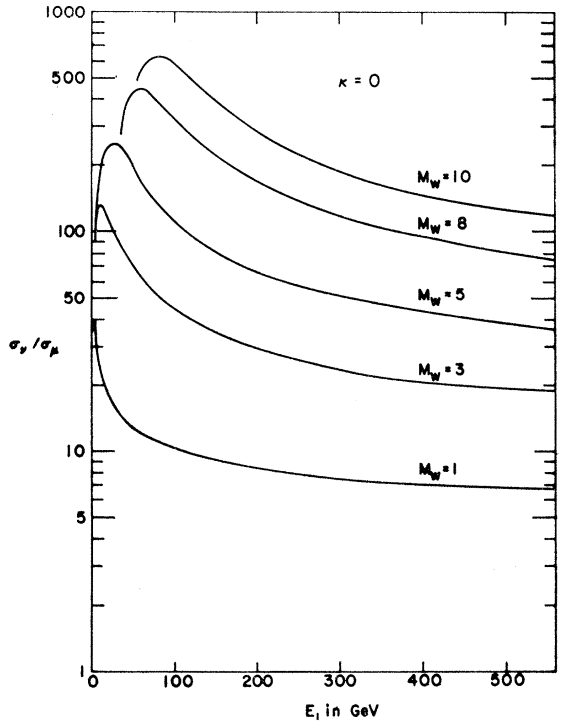

FIG. 11. Values of the ratio σ_ν/σ_μ for scattering off of protons with dipole form factors for boson masses of $M_W=1$, 3, 5, 8, and 10 GeV/c^2. Also, $\kappa=0$.

We have carried out the computations for more or less the same sets of (E_1,M_W,κ) that were considered in Secs. IV A and V B, i.e., the nucleon motion and exclusion principle are treated in order that the incoherent nuclei cross sections can be estimated. These results are listed along with those from the neutrino reaction in Tables I–III. We have also added the analogous muon curves to those neutrino figures which show the effects of varying κ (Fig. 4), and which show the change wrought by the nuclear motion and exclusion effects (Fig. 10). Figure 5 displays $d\sigma/d|T|$ for the muon off of a proton for $M_W=5$ GeV/c^2, $E_1=50$ GeV, and $\kappa=0$. Finally, Figs. 7 and 8 show the incoherent contributions of the proton and neutron for $M_W=3$ and 8 GeV/c^2 with $\kappa=0$. Our free-proton calculations are in excellent agreement with Ref. 7.

A general conclusion drawn from the numbers and curves is that for $40\leq E_1\leq 400$ GeV and $3\leq M_W\leq 15$ GeV/c^2, the muon results are smaller by two orders of magnitude on the average—this factor diminishing for larger energies at the same M_W and increasing for larger masses at a given E_1. Both $\kappa=\pm 1$ correspond to larger cross sections than $\kappa=0$ in agreement with the low-energy calculations (albeit coherent) by Überall.[6]

B. Nuclei Targets

Strictly speaking, we have the very low threshold of $E_1=M_W$. But as in the neutrino reaction, the nuclei form factors cut off the cross sections drastically at the corresponding large momentum transfers so that the coherent is dominated by the incoherent until quite a bit above threshold.

Our procedure in this part of the calculation is again the same as in the neutrino program, Sec. IV B. The target mass M_∞ is considered much larger than anything else; on the other hand, there is practically no change in our results if the actual nuclei target mass is used. In the static limit, (6.4) yields

$$\left\{\begin{matrix}|T|_{\max}\\ |T|_{\min}\end{matrix}\right\}=2|\mathbf{k}_1|^2[1-\tfrac{1}{2}F'_{\min}/|\mathbf{k}_1|^2 \pm(1-F'_{\min}/|\mathbf{k}_1|^2)^{1/2}], \quad (6.7)$$

to be compared with (4.10).

To Tables I–III are added the muon coherent results for neon, iron, and uranium. Also we illustrate the energy dependence of the neon and uranium cross sections for $M_W=3$ and 8 GeV/c^2 in Figs. 7 and 8. The qualitative statements that were made in Sec. VI A apply here. An even greater discrepancy is found between these results and the analogous neutrino calculations—as much as three orders of magnitude difference in many cases.

C. Inelasticity

We apply the same fit (5.9) to the muon reaction in order to estimate the deep-inelastic contribution to reaction (1.3). The three-dimensional integral arising in the cross section,

$$d^3\sigma=\frac{1}{2}\frac{1}{32\pi}\left(\frac{\alpha g_W}{\mathbf{k}_1 M_p}\right)^2 dW^2 d|T|\,dS'\frac{S'-1}{S'} \times\mathcal{G}_\mu^{\text{inel}}(S,T,S',W^2), \quad (6.8)$$

has the limits given by (6.3), (6.4) and

$$W_{\max}=(\sqrt{S})-M_W, \qquad W_{\min}=M_W+m_\pi. \quad (6.9)$$

We refer back to Sec. V A for a description of the calculation and only remark that the question we try to answer is with respect to the importance of such a contribution compared with our nucleon contributions.

Our findings are that (deep) inelasticity leads to roughly the same cross-section values as the single-proton final state. This can be seen in Tables I–III and in Fig. 9 which displays the four cases: neutrino and muon, elastic and inelastic. Thus there is yet an average difference of two orders of magnitude between the neutrino and muon cross sections off of protons when the estimated inelastic contributions are added.

D. Discussion of Neutrino and Muon Difference

It is clear from the start that we would not expect the same cross-section values at a given beam energy for the

neutrino and muon reactions. Besides the spin average factor of one-half for the initial muon, the propagators in Figs. 1(a) and 1(c) have different momentum dependence. On the other hand, the approximate equality of phase space and the appearance, in both cases, of essentially the same boson-photon interaction [see Figs. 1(b) and 1(d)] would seem to say that these values would not be terribly different.

A closer look reveals that an important enhancement of the neutrino cross section over the muon cross section can occur for nonasymptotic beam energies. This arises because the virtual muon in Fig. 1(a) can get *much* closer to its mass shell than the corresponding virtual muon in Fig. 2(a). The propagator denominator F in the former case vanishes as T does (neglecting μ^2) when the W is parallel to the neutrino in the $W\mu$ c.m. system. However, $F' \geq M_W{}^2-\mu^2$ in the latter case and, moreover, $|B| \geq M_W{}^2$ in both reactions. Therefore, of the four diagrams in Fig. 1, the final-state muon electromagnetic interaction stands out until we get to sufficiently large energies (where the W and μ begin to share the energy more equally).

In detail, when $\mathbf{k} \| \mathbf{k}_1$ in the $W\mu$ c.m. system, one can show that

$$F=(M_W{}^2/S')T+O(\mu^2). \tag{6.10}$$

Furthermore, F is generally small; in the laboratory frame,

$$F=-2E_2(-T)^{1/2}\cos\theta_{k_2q}+O(T,\mu^2). \tag{6.11}$$

Therefore, since E_2/E_k is very small (it is μ/M_W at $|T_{\min}|$) in the region of interest, $|F| \ll M_W{}^2$ on the average. Provided the numerators are comparable in the two reactions, this displays the origin of the difference. That the numerators are of the same order follows from gauge invariance: The $\boldsymbol{k}_2/F$ and $\boldsymbol{k}_1/F'$ parts of the neutrino and muon matrix elements cancel with the k/B boson term. As a result, the denominator differences *are* crucial since the numerators in each matrix element are effectively terms in q.

We can now explain the general features of our results in terms of the previous remarks. First of all, the ratio σ_ν/σ_μ increases with M_W for a given energy if we are not too close to threshold, as seen in Fig. 11; for a free proton with $\kappa=0$, the relation is almost linear. Next, for a given M_W, the ratio decreases with an increase in E_1, except near threshold where the size of $|T|$ is significant. Presumably there will be a slow asymptotic decrease to a factor of 2 (from the spin average). This is illustrated in Figs. 11 and 12.

The ratios for the coherent calculation are much larger and drop more slowly with larger E_1, since the nuclear form factors limit the q^2 region even more severely to the minimum values. Here E_2/E_k increases very slowly as a result and $|F|$ remains much smaller than $\frac{1}{2}M_W{}^2$ until even higher energies. We refer to the iron curve at $M_W=5$ in Fig. 12 as an illustration of this.

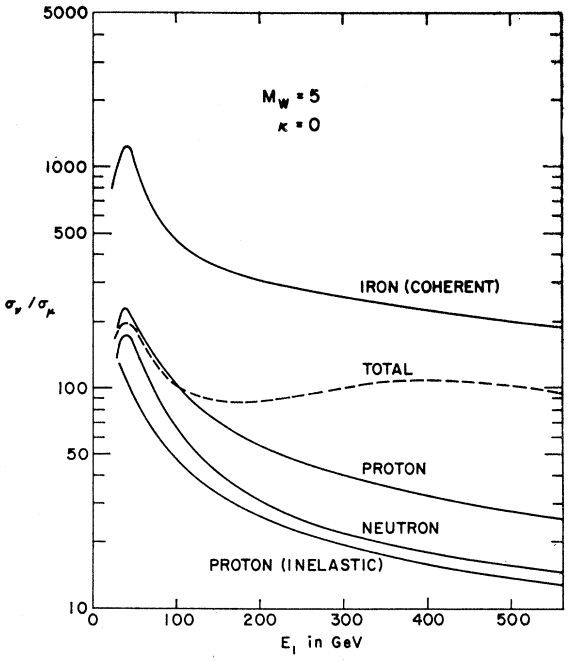

FIG. 12. Values of the ratio σ_ν/σ_μ for scattering off of protons and neutrons (with Pauli principle in the form factor), protons with inelastic form factors, and iron with Fermi form factors. The dashed curve shows the ratio for the total cross sections calculated according to Eq. (5.13). Here, $M_W=5$ GeV/c^2 and $\kappa=0$.

It was important to see if the inelastic contributions would show this large ratio since they might swamp the elastic channels via the milder form factor. Although the larger-q^2 region is not cut off here, the propagator enhancement mechanism continues to be important—an inelastic ratio plot in Fig. 12 still shows a factor of 10–100 in our energy region. Furthermore, the deep-inelastic channels do not swamp the elastic according to our results.

Finally we note that at the higher energies where the nucleon elastic and inelastic ratios begin to drop to approximately 10, the coherent cross section is dominant. Since the difference remains at two orders of magnitude for $E_1 \lesssim 1000$ GeV in the coherent case, the total cross sections for (1.1) and (1.2) off of any nucleus appear to remain a factor of 100 apart. The total cross sections, calculated according to Eq. (5.13) for iron in the two reactions, lead to the ratio curve shown in Fig. 12.

The error made in averaging over the muon spins makes matters even worse for reaction (1.3). Since the higher-energy muons from pion decay in flight have the wrong helicity for the initiation of W production, the muon's energy advantage over the neutrino is further vitiated.[19]

VII. CONCLUSIONS

We have endeavored in this first paper to give a reasonable estimate of the neutrino and muon dissociation into W bosons via an electromagnetic recoil from

various nuclei at the NAL energies. In order to analyze its experimental signature, the spectra of the W and the "prompt" muon in (1), a study of the W polarization and the spectra of its decay muon [cf. (1.2)] will be presented later.[39]

It is interesting that the muon propagator enhancement of reaction (1.1) over (1.3) led to an average difference of two orders of magnitude in all effects and channels considered as far as the NAL region of interest is concerned. There is still an order-of-magnitude difference even if we take into account the energy advantage of the muon beams provided by pion decays.[19] This means, in particular, that even for those M_W too large to be produced by a given neutrino energy, initial muons of two or three times this energy will see extremely small cross sections.

We have not looked at the problem of the Coulomb field correction[40] for the final-state muon in (1.1). As mentioned in Ref. 2, this may be important and might change the total neutrino cross section significantly. The recent calculations of Nachtmann[41] indicate a correction of order $Z\alpha/[E_\mu\times(\text{nuclear radius})]$ in the reaction $\nu_\mu+Z\to\mu^-+Z'$.

After completion of this work we received a detailed total cross-section study of reaction (1.1) performed by Chen,[42] pertaining to cosmic-ray analysis and "standard rock" nuclei. His work on the incoherent cross sections paralleled ours and his results are consistent with the results presented here. Moreover, he considered the $N^*(1236)$ channel and found that, indeed, its contribution was never more than 20% of the proton-channel cross section. On the other hand, if final-state pions are not significantly vetoed in a given experiment, such a contribution is on the same level as the neutron cross section. This should give some indication of the size of effects not included in our work.

Note added in proof. Since the completion of our manuscript, we have received two relevant papers. Berends and West [F. A. Berends and G. B. West, this issue, Phys. Rev. D **3**, 262 (1971)] have exhibited the difference between muon and neutrino W production by way of a scalar model in covariant Weizsäcker-Williams approximation. Reiff [J. Reiff, Nucl. Phys. **B23**, 387 (1970)] has performed neutrino and muon calculations for $M_W=3$ and 6 GeV which are in good agreement with our results.

ACKNOWLEDGMENTS

We thank C. N. Yang for introducing us to this problem. We benefited greatly from many discussions with A. K. Mann concerning the experimental aspects of this work. Thanks are also due to R. L. Schult for useful conversations and R. H. Hobbs for a careful reading of the manuscript.

APPENDIX

We describe here the way in which the integrals over $\mathbf{k}_2$ and $\mathbf{k}$ were performed for both reactions (1.1) and (1.3). Since most of the calculation was handled by combining Veltman's CDC 6600 algebraic program with our own FORTRAN numerical integration routine, the description here is mostly that of work the computer has done for us.

The expression for $\mathfrak{F}$ [Eq. (2.5)] is the input. After taking the trace and substituting in terms of our set of independents (2.16), a lengthy intermediate result for the neutrino reaction is obtained:

$$\mathfrak{F}(T,U,F,B,N)$$

$$=G_1\Big[\frac{1}{T}\Big(-\frac{16}{FB}-\frac{8B}{F}-\frac{16}{F}-\frac{10F}{B}+2F-\frac{2F^2}{B^2}+\frac{2F^2}{B}-\frac{16}{B^2}-\frac{16}{B}+B-15\Big)+T\Big(\frac{1}{B^2}+\frac{1}{B}\Big)-\frac{8}{F^2}-\frac{16}{FB}$$
$$+\frac{2F}{B^2}-\frac{2F}{B}-\frac{2}{B^2}+\frac{12}{B}+2\Big]+G_2\Big[\frac{1}{T^2}\Big(-\frac{16U^2}{F^2}+2U^2+\frac{32UM^2}{F^2}-\frac{32UN}{FB}+\frac{16U}{F}+\frac{4UFN}{B}-2UF-4UM^2$$
$$-\frac{16M^4}{F^2}+\frac{32NM^2}{FB}-\frac{16BM^2}{F}-\frac{16M^2}{F}-\frac{4FNM^2}{B}-\frac{24FM^2}{B}+2FM^2+\frac{2F^2N^2}{B^2}-\frac{8F^2M^2}{B^2}-\frac{2F^2N}{B}$$
$$+\frac{1}{2}F^2-\frac{16N^2}{B^2}+\frac{16N}{B}+2BM^2-30M^2+2M^4-4\Big)+\frac{1}{T}\Big(-\frac{16U^2}{FB}-\frac{8U^2}{B^2}+\frac{4U^2}{B}-\frac{16U}{F^2}+32\frac{UN}{FB}$$
$$+\frac{32UM^2}{FB}+\frac{4UFN}{B^2}+\frac{8UF}{B^2}-\frac{4UF}{B}+\frac{8UN}{B^2}+\frac{16UM^2}{B^2}-\frac{4UN}{B}-\frac{8UM^2}{B}+\frac{16U}{B}+2U-\frac{32NM^2}{FB}$$

[39] R. W. Brown, R. H. Hobbs, and J. Smith (unpublished).
[40] M. Veltman, Physica **29**, 161 (1963).
[41] O. Nachtmann, Nucl. Phys. **B18**, 112 (1970). It is asserted here, however, that a typical correction is less than 5% for uranium and $E_\mu>1$ GeV. We thank J. Cruncher for pointing out this reference to us.
[42] H. H. Chen, Nuovo Cimento **69**, A585 (1970). We thank Dr. Chen for sending these results to us.

$$-\frac{16N}{FB}-\frac{16N^2}{FB}-\frac{32M^2}{FB}-\frac{16M^4}{FB}+\frac{4B}{F}+\frac{8}{F}-\frac{4FNM^2}{B^2}-\frac{4FN}{B^2}-\frac{4FN^2}{B^2}+\frac{4FN}{B}+\frac{4FM^2}{B}+\frac{2F}{B}-F$$
$$-\frac{2F^2N}{B^2}+\frac{F^2}{B}-\frac{8NM^2}{B^2}+\frac{2N^2}{B^2}-\frac{16M^2}{B^2}-\frac{8M^4}{B^2}+\frac{4NM^2}{B}-\frac{16N}{B}+\frac{2N^2}{B}-\frac{4M^2}{B}+\frac{4M^4}{B}-\frac{B}{2}+2M^2+7.5\Big)$$
$$+T\Big(\frac{2U}{B^2}-\frac{4}{FB}-\frac{F}{B^2}-\frac{2N}{B^2}-\frac{2M^2}{B^2}-\frac{2.5}{B^2}+\frac{1}{2}\frac{1}{B}\Big)+T^2\frac{1}{2}\frac{1}{B^2}+\frac{2U^2}{B^2}-\frac{16U}{FB}-\frac{2UF}{B^2}-\frac{4UN}{B^2}-\frac{4UM^2}{B^2}$$
$$-\frac{8U}{B^2}+\frac{4U}{B}+\frac{16N}{FB}+\frac{16M^2}{FB}+\frac{8}{FB}+\frac{4FN}{B^2}+\frac{2FM^2}{B^2}+\frac{2F}{B^2}-\frac{2F}{B}+\frac{F^2}{2B^2}+\frac{4NM^2}{B^2}+\frac{4N}{B^2}+\frac{2N^2}{B^2}+\frac{10M^2}{B^2}$$
$$+\frac{2M^4}{B^2}+\frac{4}{B^2}-\frac{2N}{B}-\frac{2M^2}{B}+\frac{5}{B}-\frac{1}{2}\Big], \quad \text{(A1)}$$

where the muon mass was neglected[43] and the κ terms omitted.[44] Here, $M_W=1$ and for the proton case, $M=M_p$ and [cf. Eq. (2.6)]

$$G_1\equiv G_M{}^2,$$
$$G_2\equiv[G_E{}^2+\tau G_M{}^2]/(1+\tau). \quad \text{(A2)}$$

For the muon reaction, one need only make the replacements $U\to S$, $F\to F'$. The trace for the deep-inelastic estimates is somewhat lengthier but again easily handled.[44]

The integration over $d\Omega_k$ in (3.1) thus involves an array of integrals each of the form (recall we are in the $W\mu$ c.m. frame)

$$I(l,m,n)=\frac{1}{4\pi}\int_{-1}^{1}d\cos\theta_k\int_0^{2\pi}d\phi_k F^l B^m N^n \quad \text{(A3)}$$

for various integers l, m, and n. In terms of B and N,

$$U=2M_p{}^2+\mu^2-S-\tfrac{1}{2}(T+B)+N+\Delta, \quad \text{(A4)}$$

and in terms of θ_k and ϕ_k,

$$F=T+2q^0E_2+2|\mathbf{q}||\mathbf{k}|\cos\theta_k,$$
$$B=T+2q^0E_k-2|\mathbf{q}||\mathbf{k}|\cos\theta_k, \quad \text{(A5)}$$
$$N=p^0E_k-|\mathbf{k}|(p_x\sin\theta_k\cos\phi_k+p_z\cos\theta_k).$$

Of course, the situation is simpler in the muon case since S and $F'=S'-\mu^2$ are independent of these angles.

The assortment (A3) were done by hand in a straightforward manner; the special-frame results were made covariant with the following substitutions:

$$E_k=\begin{cases}(S'-\mu^2+1)/2E', & \nu\\ (S'+1)/2E', & \mu\end{cases}$$
$$|\mathbf{k}|=(E_k{}^2-1)^{1/2};$$
$$E_2=E'-E_k,$$
$$|\mathbf{k}_2|=|\mathbf{k}|;$$
$$q_0=\begin{cases}-(S'+T)/2E', & \nu\\ -(S'-\mu^2+T)/2E', & \mu\end{cases} \quad \text{(A6)}$$
$$|\mathbf{q}|=(q_0{}^2-T)^{1/2};$$
$$p_0=\begin{cases}[S-W^2-\frac{1}{2}(S'-T)]/E', & \nu\\ [S-W^2-\frac{1}{2}(S'+\mu^2-T)]/E', & \mu\end{cases}$$
$$|\mathbf{p}|=(p_0{}^2+T-2M_p{}^2-2W^2)^{1/2},$$
$$p_z=(p_0q_0-\Delta)/|\mathbf{q}|,$$
$$p_x{}^2=\mathbf{p}^2-p_z{}^2.$$

These have been generalized to include the inelastic as well as the muon elastic cases. Nowhere do we need the sign of p_x and everything now is a function of S, T, and

$$S'\equiv(k+k_2)^2\equiv E'^2. \quad \text{(A7)}$$

The result of the $\mathbf{k}_2$ and $\mathbf{k}$ integrals thus imply the $\mathcal{G}$'s mentioned in Eqs. (3.4), (5.1), (6.6), and (6.8).

[43] Our calculations have been done keeping all μ^2 terms. However, one can neglect these terms in the region considered by us with the resulting changes only of order 1%. This is presumably due to the fact that $\mu^2<M_p{}^2$, $M_W{}^2$, the fact that the important small-T region is characterized not by $|T|_{\min}$ but rather by something between $|T|_{\min}$ and the form-factor cutoff, and the fact that the terms in each order of μ^2 must undergo some cancellation themselves, according to Sec. IV.

[44] The complete trace with all masses and κ terms is available upon request.